

Hydrogen bond dynamics at the glass transition

U. Buchenau*

*Forschungszentrum Jülich GmbH, Jülich Centre for Neutron Science (JCNS-1)
and Institute for Complex Systems (ICS-1), 52425 Jülich, GERMANY*

(Dated: September 20, 2021)

The glass transition in hydrogen-bonded glass formers differs from the glass transition in other glass formers. The Eshelby rearrangements of the highly viscous flow are superimposed by strongly asymmetric hydrogen bond rupture processes, responsible for the excess wing. Their influence on the shear relaxation spectrum is strong in glycerol and close to zero in PPE, reflecting the strength of the hydrogen bond contribution to the high frequency shear modulus. An appropriate modification of a recent theory of the highly viscous flow enables a quantitative common description of the relaxation spectra in shear, linear and non-linear dielectrics, and heat capacity.

PACS numbers: 78.35.+c, 63.50.Lm

At the glass transition [1–4], hydrogen bonds [5, 6] have specific dynamics, always at the beginning and sometimes also at the end of the flow process: at long times, in the monoalcohols [7], the hydrogen bond decay is a Debye process, with a relaxation time much longer than the terminal shear relaxation time τ_c , so the hydrogen bond connection memory survives the breakdown of rigidity, similar to the case of polymers [8].

At short times, two peculiarities seem to appear exclusively in hydrogen-bonded glass formers, namely strongly asymmetric double-well potentials in the recoverable part of the flow relaxation [9, 10] and the excess wing at very short relaxation times [10–12]. Both features have very recently been shown to be absent in several non-hydrogen-bonding glass formers by combining mechanical data in the glass phase at many different frequencies from the literature [13].

The first clear evidence for strongly asymmetric double-well potentials in hydrogen-bonded substances appeared in an aging experiment [9]. An average asymmetry of $3.8 k_B T_g$ is needed to explain the intensity rise of the strong secondary relaxation peak dielectric signal in tripropylene glycol immediately after the initial temperature jump.

The second proof for a strong asymmetry is the strong temperature dependence $\exp(5T/T_g)$ of the excess wing measured in the glass phase of glycerol and other hydrogen bonded glass formers [10], explainable in terms of the asymmetry $\Delta = 5k_B T_g$, leading to the weakening factor $1/\cosh(\Delta/2k_B T)^2 \approx \exp(5(T - 1.52T_g)/T_g)$ for T slightly below T_g .

The present paper argues that the process behind these strongly asymmetric double-well potentials is the reversible rupture of hydrogen bonds.

The breaking of hydrogen bonds has been intensely studied in liquid water, in the water shell of biomolecules [14, 15] and at the glass transition of water-chlorine mixtures [16]. In liquid water at room temperature, a hydro-

gen bond between two water molecules has two lifetimes, a short reversible one of 0.5 ps, after which it breaks, links to another water molecule, but then returns to its former state, and a longer irreversible one of 6.5 ps [14]. Both processes are visible in the dielectric spectrum of water [17, 18], the short time process accounting for about 10 % of the total decay. Obviously, this short time process is a rupture and re-formation of the hydrogen bond leading to a metastable energy minimum lying higher than the initial one, with a high back-jump probability, precisely the kind of process needed to understand the strongly asymmetric double-well potentials in the recoverable compliance of hydrogen-bonded glass formers.

The fact that the flow relaxation in all glass formers consists of a recoverable and an irreversible part is nowadays often overlooked [1–4], but has been established unambiguously long ago by the centennial shear relaxation work of Donald Plazek [19–22]. In the shear relaxation, the irreversible part is described by the viscosity η . The reversible part consists of a Kohlrausch tail t^β (t time, β Kohlrausch exponent) of the recoverable shear compliance at times shorter than the terminal relaxation time τ_c of the viscous flow. Plazek favors the Andrade value $\beta = 1/3$. But his data do not establish β with high accuracy; more extensive investigations [23, 24] find a wide distribution of β values around 1/2.

A theoretical analysis of the reversible and irreversible shear transformation processes in the five-dimensional shear space [25–27] in terms of asymmetric double-well potentials, with the asymmetry determined exclusively by the different shear misfit of the inner Eshelby domain [28] or shear transformation zone [29, 30] in its two structural alternatives, leads to the relaxation time distribution in the barrier variable $v = \ln(\tau/\tau_c)$

$$l_{irrev}(v) = \frac{1}{3\sqrt{2\pi}} \exp(v^2) \left(\ln(4\sqrt{2}) - v \right)^{3/2} \quad (1)$$

for the irreversible processes, with $\tau_c = 8\eta/G$ (G short time shear modulus). Note that the spectrum has no Kohlrausch tail at short times; it is more like a slightly broadened Debye process around the relaxation time 1.6 τ_c , a factor of thirteen longer than the Maxwell time.

*Electronic address: buchenau-juelich@t-online.de

This terminal process is able to reproduce [27] a high quality measurement [31] of the terminal stage of the aging process in squalane, with τ_c extrapolated from shear data in the liquid phase.

The irreversible process spectrum describes dynamic heat capacity data not only in a metallic glass, but also in three hydrogen bonding substances, the vacuum pump oil PPE, glycerol and propylene glycol [25, 26], with τ_c determined from shear relaxation data of the same substances. Obviously, the additional asymmetric processes in these substances do not change the validity of eq. (1) for the irreversible flow processes. Since the irreversible processes are a continuation of the Eshelby processes of the Kohlrausch tail to relaxation times longer than τ_c , this implies that there must be a basic Kohlrausch tail in the hydrogen-bonded substances identical to the one in other glass formers.

But what obviously happens is that the basic Kohlrausch tail relaxations combine with a reversible hydrogen bond rupture, creating a double well potential with a strong additional asymmetry. This effect is bound to become stronger as the Kohlrausch tail approaches from above barrier energies close to the local hydrogen bond barriers of about 0.1 eV suggested by the picosecond scale of the hydrogen bond motion in water [14]. This is the physical reason for the excess wing and its flattening in the nanosecond region.

How does this modify the basic Kohlrausch tail? The strengthening toward lower barriers adds a logarithmic curvature, so the tail has to be described in terms of a Kohlrausch barrier density $\exp(\beta v + f_{exc} v^2)$, with a small excess wing parameter f_{exc} . The second necessary change has been already seen in the first attempt to fit hydrogen bonding spectra in terms of the theory [26]: because of the higher back-jump probability, one needs a higher Kohlrausch barrier density to achieve the viscous flow, describable in terms of a prefactor $f_K > 1$ for the Kohlrausch tail. Together, these two effects modify the theoretical equation [27] into

$$l_K(v) = f_K(1 + 0.115\beta - 1.18\beta^2)F(v) \exp(\beta v + f_{exc} v^2). \quad (2)$$

Here $F(v) \approx 1/(1 + \exp(1.19v))$ is the cutoff function of the Kohlrausch tail by the irreversible processes [27].

Having defined $l_K(v)$, one can calculate the complex shear compliance $J(\omega)$ from

$$GJ(\omega) = 1 + \int_{-\infty}^{\infty} \frac{l_K(v)dv}{1 + i\omega\tau_c \exp(v)} - \frac{i}{\omega\tau_M}, \quad (3)$$

where $\tau_M = \eta/G = \tau_c/8$ is the Maxwell time, and invert it to get $G(\omega)$.

Fig. 1 (a) shows the fit of the shear relaxation data [32] in glycerol at 196 K in terms of these equations, with the parameters compiled in Table I, demonstrating that the postulate of an additional slow mode [32] is not the only way to understand these data.

As pointed out in the theoretical paper [27], the simultaneous knowledge of irreversible and reversible relax-

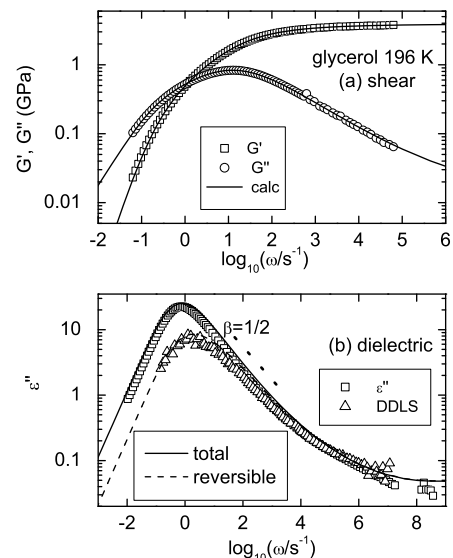


FIG. 1: (a) Measurement [32] of $G(\omega)$ in glycerol, continuous lines calculated with the parameters in Table I (b) Fit of dielectric data [33] at the same temperature with the parameters in Table II. The dashed line is calculated without the irreversible processes and happens to provide a good description of the depolarized dynamic light scattering data [11] (but see also Supplemental Material).

subst.	T	G	η	β	f_K	f_{exc}	GJ_0
	K	GPa	GPas				
glycerol	196	3.93	1.80	0.65	5.95	0.014	11.2
propylene carbonate	159	1.47	0.523	0.51	1.47	0.009	4.26
PPE	250	1.09	0.725	0.48	1	0	3.03
propylene glycol	180	4.05	0.17	0.68	5.17	0.021	10.0

TABLE I: Parameters for the theoretical description of shear relaxation data (references see text) in the four hydrogen-bonded glass formers (PPE=5-polyphenylene ether).

ation processes from the shear data implies the knowledge of all Eshelby shear relaxation processes of the substance, and enables one to judge what one sees in other relaxation techniques. The application of this concept to dielectric and adiabatic compressibility data in non-hydrogen-bonded glass formers revealed that the scheme works very well, but the dielectric and compressibility signals required the multiplication of the total spectrum with $\exp(-\tau/\tau_t)$, where τ_t is a terminal time shorter than τ_c , showing that the dielectric polarizability and the adiabatic compressibility equilibrate earlier than the terminal shear relaxation time.

In the application of the scheme to dielectric and depolarized dynamic light scattering in hydrogen bonded substances, one must multiply also the irreversible contribution of eq. (1) with f_K , because otherwise there is a discontinuity in the barrier density at τ_c . The resulting Eshelby barrier density is

$$l_E(v) = 8f_K l_{irrev}(v) + l_K(v) \exp(-\exp(v)/\tau_t). \quad (4)$$

The Debye peak in the monoalcohols [7] suggests to add a hydrogen-bond-correlation Debye decay at the time τ_t

$$l_{tot}(v) = l_D \delta(v - \ln(\tau_t/\tau_c)) + l_0 l_E(v), \quad (5)$$

where l_0 normalizes $l_E(v)$ to $1 - l_D$.

Fig. 1 (b) shows that one can describe the dielectric spectrum [33] with this recipe. However, one must adapt the excess wing parameter f_{exc} , which is a bit larger in the dielectric data. As a consequence, one must also adapt β to a slightly higher value, because the slope of the Kohlrausch tail at τ_c contains a small negative component from the diminishing influence of hydrogen bonds toward higher barriers. The five parameters $\Delta\chi$ (the difference between the dielectric susceptibilities at very low and very high frequency), f_{exc} , τ_t/τ_c , β and l_D for the dielectric data are listed in Table II.

Note that the recipe implies that the lifetime

$$\tau_{dip} = \frac{1.6\tau_c\tau_t}{1.6\tau_c + \tau_t} \quad (6)$$

of the dipole moment of an Eshelby region or shear transformation zone gets shorter than the lifetime $1.6\tau_c$ of the region itself.

subst.	T K	$\Delta\chi$	β	f_{exc}	τ_t/τ_c	l_D
glycerol	196	62.7	0.71	0.018	0.51	0.21
propylene carbonate	159	101.0	0.67	0.019	1.55	0.29
PPE	250	1.9	0.63	0.014	0.83	0.10
propylene glycol	180	64.4	0.68	0.021	81.0	0.00

TABLE II: Parameters for the theoretical description of dielectric relaxation data (references see text) in the four hydrogen-bonded glass formers.

Fig. 1 (b) shows also, as a dashed line, the calculated dielectric signal without the irreversible processes, which happens to describe the shifted depolarized dynamic light scattering data [11] very well. However, as argued by Thomas Blochowicz (see Supplemental Material), this agreement can be shown to be fortuitous.

Glycerol with its three strong oxygen hydrogen bonds per molecule has a much higher shear modulus than propylene carbonate, where the oxygen atoms do not have a hydrogen atom of their own, but link to the hydrogens bonded to carbon atoms. As a consequence, the deviation of the parameter f_K from 1 in Table I of propylene carbonate is about a factor of ten smaller than the one of glycerol, and its shear modulus is not much higher than the 1 GPa of van-der-Waals bonded molecular glass formers [26]. But otherwise, the results of the same analysis of propylene carbonate data [34] shown in Fig. 2 (a) and (b) and tabulated in Table I and II are very similar.

PPE has even weaker hydrogen bonds, so weak that one gets a perfect fit of the shear data [35] in terms of the original model with only the three parameters G , η and β in Table I, taken over from [27]. But the former

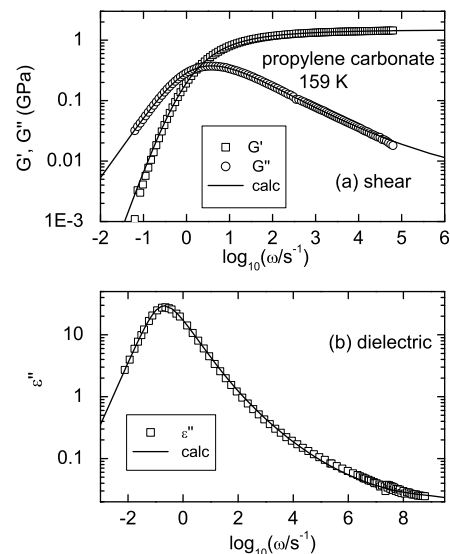


FIG. 2: (a) Measurement [34] of $G(\omega)$ in propylene carbonate at 159 K, continuous lines calculated with the parameters in Table I (b) Fit of dielectric data [34] at the same temperature in the same cryostat with the parameters in Table II.

fit of the dielectric data [27] improves markedly with the parameters of Table II, as demonstrated in Fig. 3. The excess wing parameter is about the same as in the other three substances and β changes strongly, showing that the dielectric signal is dominated by the strong hydrogen bond component which is not visible in the shear data.

The last example, propylene glycol, has again a strong hydrogen bond component in its shear data [36]. In the dielectric data [37], one finds the same f_{exc} and β as in the shear data. In this case, one does not really need τ_t ; the dielectric relaxation terminates at the value calculated from the shear data and there is no hydrogen-bond-correlation Debye decay within experimental error.

The description of dielectric data of hydrogen-bonded glass formers in terms of strongly asymmetric double-well potentials supplies a new interpretation of nonlinear dielectric data (see Supplemental Material).

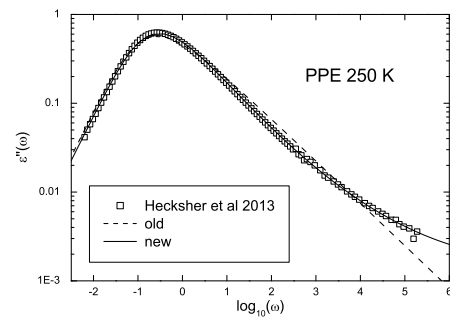


FIG. 3: (Old [27] (dashed line) and new (continuous line, parameters Table II) calculations for dielectric data in PPE at 250 K [35].

Table I compiles the parameters for the four substances, including in the last row the total recoverable compliance GJ_0 , which in glycerol is nearly a factor of four higher than in normal glass formers, showing that one needs much more recoverable processes to start the viscous flow, because of the strong back-jump tendency of the hydrogen bonds. In all four cases, the shear analysis was done over the entire temperature range of the measurements, to look for a possible temperature dependence of the parameters. f_K and f_{exc} were found to be temperature-independent within experimental accuracy. For glycerol, the temperature-dependent shear moduli agree within a few percent with those of a transverse wave Brillouin scattering determination [38], showing the high quality of both measurements.

Though one has to invoke a stronger asymmetry, the possibility to obtain good fits of high quality shear data

in hydrogen bonding substances with the two additional parameters f_K for the strength of the hydrogen bond influence and f_{exc} for the excess wing curvature supports the validity of the general theory of the highly viscous flow [27].

To summarize, one can understand the shear relaxation of hydrogen-bonded undercooled liquids close to their glass transition in a recent theory of the highly viscous flow by taking the influence of highly asymmetric reversible hydrogen bond ruptures, well studied in water, into account. The hydrogen bond ruptures make the Kohlrausch tail double-well potentials strongly asymmetric and give rise to the excess wing, absent in non-hydrogen-bonded glass formers. One can describe shear, linear and non-linear dielectric, and dynamic specific heat data consistently within the extended theory.

-
- [1] A. Cavagna, Phys. Rep. **476**, 51 (2009)
- [2] L. Berthier and G. Biroli, Rev. Mod. Phys. **83**, 587 (2011)
- [3] C. P. Royall and S. R. Williams, Phys. Rep. **560**, 1 (2015)
- [4] L. Berthier, J. Chem. Phys. **150**, 160902 (2019)
- [5] Th. Steiner, Angew. Chem. Int. Ed. **41**, 48 (2002)
- [6] V. David, N. Grinberg, and S. C. Moldoveanu, in *Advances in Chromatography Vol. 54* (Eds: E. Gruschka, N. Grinberg), CRC, Boca Raton 2018, chap. 3
- [7] R. Böhmer, C. Gainaru', and R. Richert, Phys. Rep. **545**, 125 (2014)
- [8] A. L. Agapov, V. N. Novikov, T. Hong, F. Fan, and A. P. Sokolov, Macromolecules **51**, 4874 (2018)
- [9] J. C. Dyre and N. B. Olsen, Phys. Rev. Lett. **91**, 155703 (2003)
- [10] C. Gainaru, R. Böhmer, R. Kahlau, and E. Rössler, Phys. Rev. B **82**, 104205 (2010)
- [11] J. Ph. Gabriel, P. Zourchang, F. Pabst, A. Helbling, P. Weigl, T. Böhmer, and Th. Blochowicz, Phys.Chem.Chem.Phys. **22**, 11644 (2020)
- [12] F. Pabst, J. Gabriel, T. Böhmer, P. Weigl, A. Helbling, T. Richter, P. Zourchang, Th. Walther, and Th. Blochowicz, arXiv:2008.01021
- [13] U. Buchenau, G. D'Angelo, G. Carini, X. Liu, and M. A. Ramos, arXiv:2012.10139
- [14] B. Bagchi, Chem. Rev. **105**, 3197 (2003)
- [15] D. Laage and J. T. Hynes, Science **311**, 832 (2006)
- [16] D. Corradini, M. Rovere, and P. Gallo, J. Chem. Phys. **132**, 134508 (2010)
- [17] J. B. Hasted, S. K. Husain, F. A. M. Frescura, and R. Birch, Chem. Phys. Lett. **118**, 622 (1985)
- [18] W. J. Ellison, K. Lamakaouchi, and J.-M. Moreau, J. Mol. Liq. **68**, 171 (1996)
- [19] D. J. Plazek, J. Phys. Chem. **69**, 3480 (1965)
- [20] D. J. Plazek and J. H. Magill, J. Chem. Phys. **45**, 3038 (1966)
- [21] D. J. Plazek, C. A. Bero and I.-C. Chay, J. Non-Cryst. Solids **172-174**, 181 (1994)
- [22] C. M. Roland, P. G. Santangelo, D. J. Plazek, and K. M. Bernatz, J. Chem. Phys. **111**, 9337 (1999)
- [23] R. Böhmer, K. L. Ngai, C. A. Angell and D. J. Plazek, J. Phys. Chem. **99**, 4201 (1993)
- [24] A. I. Nielsen, T. Christensen, B. Jakobsen, K. Niss, N. B. Olsen, R. Richert, and J. C. Dyre, J. Chem. Phys. **130**, 154508 (2009)
- [25] U. Buchenau, J. Chem. Phys. **148**, 064502 (2018)
- [26] U. Buchenau, J. Chem. Phys. **149**, 044508 (2018)
- [27] U. Buchenau, arXiv:2003.07246
- [28] J. D. Eshelby, Proc. Roy. Soc. **A241**, 376 (1957)
- [29] M. L. Falk and J. S. Langer, Phys. Rev. E **57**, 7192 (1998)
- [30] W. L. Johnson and K. Samwer, Phys. Rev. Lett. **95**, 195501 (2005)
- [31] K. Niss, J. C. Dyre, and T. Hecksher, J. Chem. Phys. **152**, 041103 (2020)
- [32] M. H. Jensen, C. Gainaru, C. Alba-Simionesco, T. Hecksher, and K. Niss, Phys. Chem. Chem. Phys. **20**, 1716 (2018)
- [33] S. Adichtchev, T. Blochowicz, C. Tschirwitz, V. N. Novikov and E. A. Rössler, Phys. Rev. E **68**, 011504 (2003)
- [34] C. Gainaru, T. Hecksher, N. B. Olsen, R. Böhmer, and J. C. Dyre, J. Chem. Phys. **137**, 064508 (2012)
- [35] T. Hecksher, N. B. Olsen, K. A. Nelson, J. C. Dyre and T. Christensen, J. Chem. Phys. **138**, 12A543 (2013)
- [36] C. Maggi, B. Jakobsen, T. Christensen, N. B. Olsen and J. C. Dyre, J. Phys. Chem. B **112**, 16320 (2008)
- [37] C. Leon, K. L. Ngai, and C. M. Roland, J. Chem. Phys. **110**, 11585 (1999)
- [38] F. Scarponi, L. Comez, D. Fioretto, and L. Palmieri, Phys. Rev. B **70**, 054203 (2004)

Supplemental Material: Hydrogen bond dynamics at the glass transition

U. Buchenau*

Forschungszentrum Jülich GmbH, Jülich Centre for Neutron Science (JCNS-1)
and Institute for Complex Systems (ICS-1), 52425 Jülich, GERMANY

(Dated: September 20, 2021)

The argument of Thomas Blochowicz for the depolarized dynamical scattering is presented and discussed. The consequences of the main paper for the nonlinear dielectric effects are worked out.

PACS numbers: 78.35.+c, 63.50.Lm

I. DEPOLARIZED DYNAMICAL LIGHT SCATTERING: BLOCHOWICZ ARGUMENT

The imaginary peak of the depolarized dynamical light scattering data in glycerol lies a factor of three higher than the one of the dielectric data [1]. In an earlier draft [2] of the present paper, this led to the hypothesis that one sees only reversible relaxations in the depolarized dynamical light scattering.

In a discussion with the Author, Thomas Blochowicz pointed out that one could check the hypothesis in DC704, where the two peaks happen to coincide [3].

This is done in Fig. 1, which shows the dielectric spectrum [4] of DC704 and its fitted [5] full and reversible parts, with a reversible part peak frequency a factor of 2.5 higher than the one of the full spectrum.

The comparison to the measured depolarized dynamical light scattering data of DC704 [3] shows clearly that the former hypothesis of the Author is wrong. In fact, the hypothesis has the additional weakness that, according to theory [6], at the crossover from reversible to irreversible structural transitions their nature does not change, so their visibility in the depolarized dynamic light scattering should not change.

Looking for an alternative explanation of the upwards peak shift from dielectrics to depolarized dynamical light scattering in glycerol, one remembers that for the simple case of isotropic rotational diffusion of a molecular dipole Debye [7] predicts the peak in ϵ'' at $\omega = 2D_r$ (D_r rotational diffusion constant) and Berne and Pecora [8] predict the imaginary peak in the depolarized dynamical light scattering at $\omega = 6D_r$, a factor of three higher.

Naturally, the molecular motion in the α -relaxation of glycerol is not a simple rotational diffusion. On the other hand, the terminal stage of the motion at the time τ_t , where the many Eshelby transitions in which the molecule participated have removed its initial connection to its neighbors, is essentially a small-angle motion according to NMR evidence [9]. So the measured peak shift in glycerol [1] seems understandable, even quantitatively.

But this poses the question why the peak shift is not observed in DC704 [3].

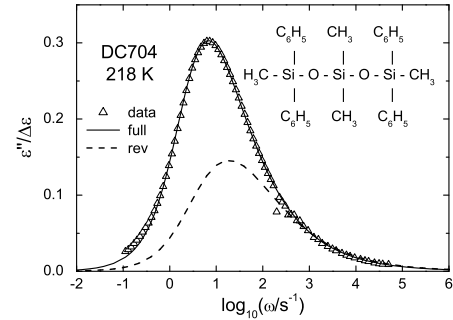


FIG. 1: Dielectric data [4] in DC704 at 218 K, together with their theoretical fit [5] (continuous line). Taking only the reversible processes to be responsible for the depolarized dynamical light scattering, one predicts the dashed line with a peak shift which is not observed in experiment [3]. The structure of DC704 with its two Si-O-Si bonds in the center is shown in the upper right side of the figure.

To understand this, look at the structure of the DC704 molecule in Fig. 1, with its two very flexible Si-O-Si bond bending degrees of freedom. The dipole moment of each of them is given by the displacement of the oxygen atom from the line connecting the two silicon atoms. One does not expect the very large DC704 molecule to rotate much during the whole α -process, but the Si-O-Si dipole moments will change in every Eshelby transition in which the molecule participates. If one idealizes each Si-O-Si bond as a dipole making large jumps in a fixed plane perpendicular to the line connecting the two silicon atoms, with a 180-degree jump equally probable as a 90-degree jump, one does indeed predict equal peak positions in dielectrics and depolarized dynamical light scattering.

II. NONLINEAR DIELECTRIC EFFECTS

The first two decades of this century have provided high quality experimental nonlinear dielectric results, all of them taken close to the glass transition in hydrogen-bonded undercooled liquids [10–24]. These data hold the promise for a deep insight into the nature of the highly viscous flow - if one could understand them.

Previous attempts [17, 25] to explain the experimental findings in terms of the nonlinear dielectric response of

*Electronic address: buchenau-juelich@t-online.de

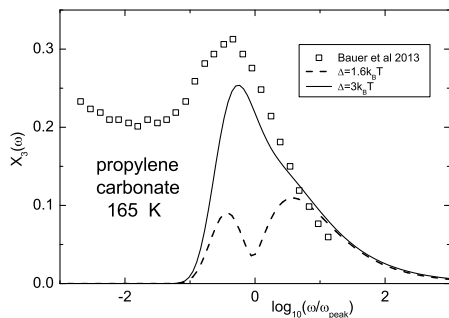


FIG. 2: Measurement of the hump in the nonlinear dielectric effect at 3ω in propylene carbonate at 165 K [20], compared to theoretical fits with the average asymmetry $\Delta = 1.6k_B T_g$ and $\Delta = 3k_B T_g$. Parameters of the fit with $\Delta = 3k_B T_g$ listed in Table I.

asymmetric double-well potentials [18, 26] were not very successful, but Ranko Richert's phenomenological model [10, 12–14, 16, 23], sometimes also called box model, is impressively able to explain all nonlinear dielectric findings without free parameters. The model requires the hole-burning assumption [27] that the relaxations heat up into a different state when they absorb the electric energy.

The results of the present paper enable a new interpretation of the Richert model in terms of asymmetric double-well potentials, attributing the energy absorption to a reduction of the asymmetry Δ .

Experimentally [14], one finds that the energy absorption plays a large role in the nonlinear change of $\epsilon''(\omega)$, but does not influence the nonlinear signal at 3ω . Therefore one has to begin with an analysis of the average asymmetry Δ and the dipole moment change M of the Eshelby transitions from the third order nonlinear susceptibility $\chi_3^{(3)}(\omega)$, expressed in a convenient dimensionless form [17]

$$X_3(\omega) = \frac{NkT}{\epsilon_0 \Delta \chi^2} \left| \chi_3^{(3)}(\omega) \right|. \quad (1)$$

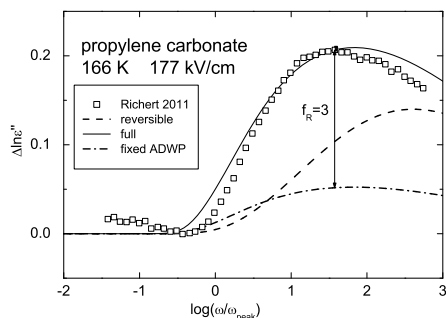


FIG. 3: Fit of measured nonlinear $\Delta\epsilon''$ -data [16] in propylene carbonate in terms of a Richert factor of three and an average asymmetry $3k_B T_g$. A fit with only reversible Eshelby transitions can again be excluded.

Here N is the number density of molecules, and $\Delta\chi$ is the susceptibility difference between low and high frequencies.

For a constant asymmetry density, and weighting the asymmetries with the prefactor $1/\cosh^2(\Delta/2k_B T)$ (the weakening factor for the relaxation strength of an asymmetric double well potential), one expects the average value $\Delta/k_B T = 1.317$, the one which fulfills the condition [26] for a hump in $X_3(\omega)$. In the hydrogen-bonding glass formers, one expects a larger value, though maybe at the flow process markedly smaller than the $5 k_B T$ found for the excess wing in the glass phase [28].

Fig. 2 shows a measurement of $X_3(\omega)$ in propylene carbonate at 165 K [20], together with two fits in terms of the theoretical barrier density of the main paper, one for $\Delta = 1.6k_B T$ and the other for $\Delta = 3k_B T$. The first one is close to the hump condition $\tanh(\Delta/2k_B T)^2 = 1/3$, where one has strong frequency oscillations in the nonlinear signal [26]. The deep dip in the calculated curve is due to the interference effects from neighboring relaxations. At $\Delta = 3k_B T$, the oscillations are much less pronounced and lead only to a weak shoulder, much more consistent with the measured data. Both fits required the assumption of a negligible nonlinear signal from the excess wing, in order to get the right slope at high frequencies. One has a low-frequency cutoff $\exp(-1/\omega\tau_{dip})$, with $\tau_{dip} = 1.6\tau_c\tau_t/(1.6\tau_c + \tau_t)$, from the lifetime of the dipole of the Eshelby regions defined in the main paper.

The fit with $\Delta = 3k_B T$ required a dipole moment change $M/\mu = 2.07$ in the Eshelby transitions, where $\mu = 5.67$ D is the dipole moment calculated from $\Delta\chi$ and the density at 166 K [16], a Kirkwood factor 1.16 larger than the molecular dipole moment of the isolated molecule.

Knowing Δ and M from the fit of $X_3(\omega)$, one is able to calculate (again with the same lifetime limitation as before) the nonlinear change $\Delta\epsilon''$ of the imaginary part of $\epsilon''(\omega)$ under the influence of a strong alternating electric field for fixed asymmetric double-well potentials [26] (the dot-dashed line in Fig. 3), which turns out to be a factor of four lower than measured propylene carbonate data [16].

In the spirit of the Richert model, we attribute this enhancement to a change of the relaxation under the influence of the strong alternating field. But instead of postulating a transformation of the relaxation into one at higher temperature, we merely assume a decrease of the asymmetry Δ . For an asymmetry $3k_B T$, one only needs a decrease by less than $0.2 k_B T$ to achieve the measured [16] enhancement in an alternating field of 177 kV/cm.

We quantify this Richert enhancement $1 + f_R$ by the Richert factor f_R , in the case of Fig. 3 $f_R = 3$.

An important question is whether the effect is limited to reversible transitions in asymmetric double-well potentials. The dashed line in Fig. 3 is obtained if one limits the barrier density to the reversible part $l_K(v)$ of the shear relaxation and is obviously too low to explain

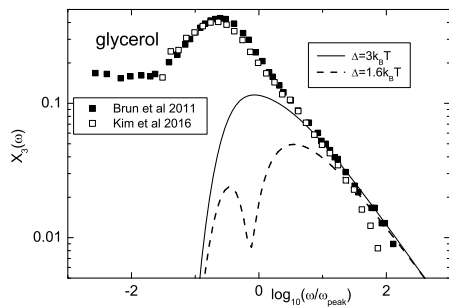


FIG. 4: Measurements of the hump in the nonlinear dielectric effect at 3ω in glycerol at 204.7 K [17] (full squares) and at 210 K [23] (open squares), compared to theoretical fits with the two average asymmetries $\Delta = 1.6k_B T_g$ and $\Delta = 3k_B T_g$. Parameters of the fit with $\Delta = 3k_B T_g$ listed in Table I.

the data. One also needs the Eshelby transitions which are irreversible in the shear relaxation. But since the asymmetry in the double-well potentials seen in the dielectric signal seems to be considerably higher than in those seen by the shear relaxation (at least in propylene carbonate, which is not far from a normal van der Waals molecular glass former), it seems possible that one still deals with reversible transitions. A second possibility is that the irreversible Eshelby transitions have the same average asymmetry and obey the theoretical equations [18, 26] for the nonlinear signal of asymmetric double-well potentials.

For $\chi_3^{(3)}(\omega)$, the postulated decrease of the average asymmetry Δ causes an increase by the factor 1.15 from the increased relaxation strength, and a decrease by the factor 0.9 from the dip effect in Fig. 2, practically no change, thus justifying the fixed-potential assumption for the theoretical description of $X_3(\omega)$.

Figs. 4 and 5 show the similar results of the same procedure for glycerol. In this case, the Richert factor equals 2, and the low-frequency cutoff has to be calculated with $1.8\tau_{dip}$ (in glycerol, shear [29] and dielectric data [30] were not done on the same sample and in the

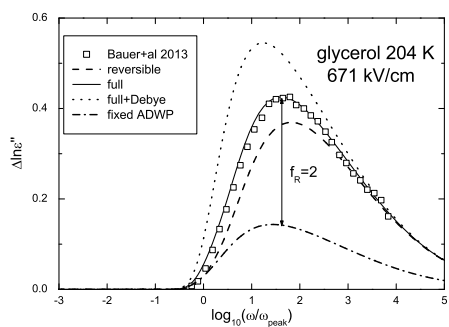


FIG. 5: Fit of measured nonlinear $\Delta \epsilon''$ -data [19] in glycerol in terms of a Richert factor of two and an average asymmetry $3k_B T_g$. Fits with possibilities to be excluded are also shown.

same cryostat, so τ_{dip} is not so accurately determined as in propylene carbonate). The results corroborate those in Fig. 2 and 3. Fig. 5 contains one more calculated curve, the dotted one for the case that also the terminal Debye process contributes, showing that one can exclude that.

Fig. 6 shows that the propylene carbonate parameters in Table I are able to describe time-dependent on-switching and off-switching experiments of the strong alternating field [16], merely assuming that the fixed potential component relaxes exponentially with the relaxation time of the potential, while the Richert component relaxes with the Kohlrausch function $\exp(-(t/1.6\tau_c)^\beta)$. In the off-switch, one has to take into account that the Kohlrausch function is not fully saturated (in the case of Fig. 6 only to 94 percent). One can take the effect approximately into account by replacing $\exp(-(t/1.6\tau_c)^\beta)$ for the off-switch by $(\exp(-(t/1.6\tau_c)^\beta) - 0.06)/0.94$, which describes the terminal data in Fig. 6 reasonably well.

subst.	T	$\Delta\chi$	μ	M/μ	E_e	f_R
	K		D		kV/cm	
propylene carbonate	166	130.0	5.67	2.07	177	3.0
glycerol	204.7	62.7	4.26	1.70	671	2.0

TABLE I: Parameters for the theoretical description of nonlinear dielectric relaxation data (references see text) in the two hydrogen-bonded glass formers for an assumed average asymmetry $\Delta = 3k_B T$.

To conclude, the hydrogen bond scheme of the main paper is able to supply a quantitative description of nonlinear dielectric data around and above the main absorption peak in term of double-well potentials with an average asymmetry of about $3k_B T_g$, nearly a factor of two lower than the value $5k_B T_g$ measured at the excess wing [28] and close to the value $3.8BT_g$ measured at the secondary relaxation peak of tripropylene glycol [31]. Reversible and irreversible transitions contribute equally, possibly because the transitions relevant for the dielectric signal remain reversible and asymmetric until one

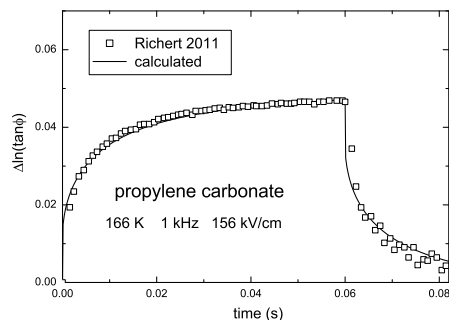


FIG. 6: Measured nonlinear on-switch and off-switch $\Delta \ln(\tan \Phi)$ -data for a strong alternating electric field in propylene carbonate [16], described in terms of the parameters in Table I.

reaches the terminal Debye decay.

The question to which extent the hump in $X_3(\omega)$ is due to the Eshelby or shear transformation zone transition, and how much comes from the terminal Debye process, remains open. Remember that the terminal Debye process has a strong hump in 2-ethyl-1-hexanol [32] and no hump in 1-propanol [21], both monoalcohols with a well-separated Debye peak and a high Kirkwood factor. Judging from the factor of three between the depolar-

ized dynamic light scattering peak frequency [1] and the dielectric one in glycerol, as well as from the NMR analysis [9] of the terminal relaxation, one would guess that in this case the terminal Debye process does not contribute to the hump, but should follow the Debye description [33]. The same explanation is suggested for propylene carbonate by the theoretical calculation in Fig. 2, which together with a Debye contribution seems to be able to explain the hump quantitatively.

-
- [1] J. Ph. Gabriel, P. Zourchang, F. Pabst, A. Helbling, P. Weigl, T. Böhmer, and Th. Blochowicz, *Phys. Chem. Chem. Phys.* **22**, 11644 (2020)
- [2] U. Buchenau, arXiv:2105.06394v2
- [3] F. Pabst, J. Ph. Gabriel, T. Böhmer, P. Weigl, A. Helbling, T. Richter, P. Zourchang, Th. Walther, and Th. Blochowicz, *J. Phys. Chem. Lett.* **12**, 14 (2021)
- [4] T. Hecksher, N. B. Olsen, K. A. Nelson, J. C. Dyre and T. Christensen, *J. Chem. Phys.* **138**, 12A543 (2013)
- [5] U. Buchenau, arXiv:2003.07246
- [6] U. Buchenau, *J. Chem. Phys.* **149**, 044508 (2018)
- [7] P. Debye, *Polar Liquids*, Chem. Catalog Comp., N. Y. 1929
- [8] B. J. Berne and R. Pecora, *Dynamic Light Scattering*, Wiley-Interscience, 1976
- [9] G. Diezemann, R. Böhmer, G. Hinze, and H. Sillescu, *J. Non-Cryst. Solids* **235-237**, 121 (1998)
- [10] R. Richert and S. Weinstein, *Phys. Rev. Lett.* **97**, 095703 (2006)
- [11] S. Weinstein and R. Richert, *Phys. Rev. B* **75**, 064302 (2007)
- [12] L.-M. Wang and R. Richert, *Phys. Rev. Lett.* **99**, 185701 (2007)
- [13] W. Huang and R. Richert, *Eur. Phys. J. B* **66**, 217 (2008)
- [14] W. Huang and R. Richert, *J. Chem. Phys.* **130**, 194509 (2009)
- [15] C. Crauste-Thibierge, C. Brun, F. Ladieu, D. L'Hôte, G. Biroli, and J.-P. Bouchaud, *Phys. Rev. Lett.* **104**, 165703 (2010)
- [16] R. Richert, *Thermochimica Acta* **522**, 28 (2011)
- [17] C. Brun, F. Ladieu, D. L'Hôte, M. Tarzia, G. Biroli, and J.-P. Bouchaud, *Phys. Rev. B* **84**, 104204 (2011)
- [18] F. Ladieu, C. Brun, D. L'Hôte, *Phys. Rev. B* **85**, 184207 (2012)
- [19] Th. Bauer, P. Lunkenheimer, S. Kastner and A. Loidl, *Phys. Rev. Lett* **110**, 107603 (2013)
- [20] Th. Bauer, P. Lunkenheimer and A. Loidl, *Phys. Rev. Lett* **111**, 225702 (2013)
- [21] Th. Bauer, M. Michl, P. Lunkenheimer, and A. Loidl, *J. Non-Cryst. Solids* **407**, 66 (2015)
- [22] S. Samanta and R. Richert, *J. Chem. Phys.* **140**, 054503 (2014)
- [23] P. Kim, A. R. Young-Gonzalez, and R. Richert, *J. Chem. Phys.* **145**, 064510 (2016)
- [24] S. Albert, Th. Bauer, M. Michl, G. Biroli, J.-P. Bouchaud, A. Loidl, P. Lunkenheimer, R. Tourbot, C. Wiertel-Gasquet, and F. Ladieu, *Science* **352**, 1308 (2016)
- [25] U. Buchenau, *J. Chem. Phys.* **146**, 214503 (2017)
- [26] G. Diezemann, *Phys. Rev. E* **85**, 051502 (2012)
- [27] B. Schiener, R. Böhmer, A. Loidl, and R. V. Chamberlin, *Science* **274**, 752 (1996)
- [28] C. Gainaru, R. Böhmer, R. Kahlau, and E. Rössler, *Phys. Rev. B* **82**, 104205 (2010)
- [29] M. H. Jensen, C. Gainaru, C. Alba-Simionesco, T. Hecksher, and K. Niss, *Phys. Chem. Chem. Phys.* **20**, 1716 (2018)
- [30] S. Adichtchev, T. Blochowicz, C. Tschirwitz, V. N. Novikov and E. A. Rössler, *Phys. Rev. E* **68**, 011504 (2003)
- [31] J. C. Dyre and N. B. Olsen, *Phys. Rev. Lett.* **91**, 155703 (2003)
- [32] Th. Bauer, P. Lunkenheimer, and A. Loidl, *Phys. Rev. Lett.* **111**, 225702 (2013)
- [33] W. T. Coffey, B. V. Paranjape, *Proc. R. Irish Acad. A* **78**, 17 (1978)